Bulletin of Engineering Geology and the Environment (2020) 79:5213–5228
https://doi.org/10.1007/s10064-020-01886-9

ORIGINAL PAPER

SUSLE: a slope and seasonal rainfall-based RUSLE model for regional quantitative prediction of soil erosion

Faming Huang[1] · Jiawu Chen[1] · Chi Yao[1] · Zhilu Chang[1] · Qinghui Jiang[1] · Shu Li[2] · Zizheng Guo[3]

Received: 19 October 2019 / Accepted: 10 June 2020 / Published online: 29 June 2020

Abstract

The Revised Universal Soil Loss Equation (RUSLE) models are most widely used for quantitative prediction of soil erosion. However, these models have many shortcomings. For example, the annual total rainfall is often adopted, ignoring the inhomogeneity of seasonal rainfall. The adopted vegetation coverage indexes (VCIs) are usually the annual average vegetation coverage or VCIs obtained by monitoring on a specific day, ignoring the seasonal changes in VCIs during the year. In addition, the impact of slope on the conservation practices factor is not considered. To overcome these problem, this study aims to propose a seasonal and slope factor-based RUSLE (SUSLE) model that considers the seasonal changes in rainfall and VCIs and the effect of slope on the conservation practices factor. Based on GIS and remote sensing, the quantitative prediction of soil erosion in Ningdu County, Jiangxi Province, in 2017 is taken as a case study. The traditional RUSLE model and the proposed SUSLE model are analyzed and compared. Results show that the overall distribution characteristics of soil erosion in the two models are similar that the SUSLE model is more consistent than the RUSLE model in all erosion levels and that the prediction performances of the SUSLE model in the very low, moderate, and high erosion levels are better than those of the RUSLE model. The distribution characteristics of soil erosion in different periods and the relationships between soil erosion and environmental factors (e.g., slope and land use) under the SUSLE model are discussed. The results show that the maximum erosion area occurred in spring and the minimum area in autumn; the soil erosion amount on slopes of 8~25° reached 65.14% of the total amount; bare grassland and cultivated land are the main land cover types impacted by soil erosion in Ningdu County.

Keywords Soil erosion · Revised Universal Soil Loss Equation · Seasonal and slope-based RUSLE model · Geographic information system · Remote sensing

Introduction

Soil erosion is one of the most serious environmental problems worldwide (Liu et al. 2019; Pimentel 2006; Zhu 2014). Soil provides a material basis for all species in the ecosystem. Erosion and destruction of soil will lead to a series of ecological environmental problems, such as decreasing land productivity, deteriorating water quality, and aggravating flood disasters, which seriously restrict the sustainable development of human beings (Cao et al. 2018; Dai et al. 2019; Zhang et al. 2019). Therefore, it is necessary to study the quantitative prediction method of regional soil erosion (Kang et al. 2019; Mushi et al. 2019).

Geographic information systems and remote sensing provide an important technical basis for the quantitative prediction of soil erosion using many types of soil erosion models (de Lollo and Sena 2013; Lal 2001; Wang et al. 2019). At present, soil erosion prediction models mainly include process-based physical models and empirical models. However, it should be noted that the process-based physical models, such as the Water Erosion Prediction Project (WEPP) (Fang et al. 2019), European Soil Erosion Model (EUROSEM) (Liangsong et al., 2015), and Limburg Soil

✉ Chi Yao
chi.yao@ncu.edu.cn

Faming Huang
faminghuang@ncu.edu.cn

[1] School of Civil Engineering and Architecture, Nanchang University, Nanchang 330031, China

[2] Changjiang Institute of Survey, Planning, Design and Research co., LTD, Wuhan 430010, China

[3] Faculty of Engineering, China University of Geosciences, Wuhan 430074, China

Erosion Model (LISEM) (Baumann et al. 2020), have many limitations in that the input parameters and field-measured data are difficult to obtain and have uncertainties. These limitations make it difficult for physical models to accurately simulate the soil erosion process, and the simulations are not as extensive as those in the empirical models.

The Universal Soil Loss Equation (USLE) (Bagherzadeh 2012; Belasri and Lakhouili 2016; Kinnell 2018; Wischmeier and Smith 1978; Zhang et al. 2018; Zhu 2014) and the Revised Universal Soil Loss Equation (RUSLE) (Ganasri and Ramesh 2016; Renard et al. 1997; Shi et al. 2004) models are the empirical models most commonly used in studies to predict soil erosion due to their advantages, such as simple structure, easily acquired parameters, comprehensive consideration of factors, ability of regional soil erosion prediction, and strong practicability comparing with the physical models. Meanwhile, there are great potential that the prediction precision can be improved by both USLE and RUSLE models because of the various accurate and rich data in the study area. Although, the RUSLE model can address this problem that the USLE cannot predict soil erosion of individual rainfall events on the basis of annual erosion data (Renard et al. 1997), it cannot reflect the physical processes of soil erosion such as the separation of rainfall and runoff, and rainfall transport and runoff transport. (Cuomo et al. 2015). Among these studies, Ganasri and Ramesh (2016) used the RUSLE model to estimate the soil losses in the Nethravathi Basin in southwest India, where the influences of seasonal changes of vegetation cover on the annual cover and management factor were ignored. Zhu (2014) evaluated the soil erosion in the Danjiangkou reservoir region in China based on the USLE model. However, the uneven spatial and temporal distribution features of rainfall were not considered to calculate the rainfall erosivity factor. Fang et al. (2019) applied the RUSLE model to study soil erosion in the Yangtze River basin of Jiangsu Province, China. However, the effects of topographic slope on the conservation practices factors were not considered. Xue et al. (2018) evaluated soil erosion dynamics based on the RUSLE model in the Wangjiagou watershed in China, without considering the effects of seasonal changes of rainfall and vegetation cover on soil erosion.

When the USLE and RUSLE models are used for quantitative prediction of soil erosion, most researchers usually adopt the annual total rainfall to calculate the rainfall erosivity factor without considering the problem of uneven rainfall in each season; in the calculation of vegetation cover and management factor, the annual average or a specific day's vegetation coverage indexes (VCIs) are often used, without considering the variation in VCIs with the change in seasons (Cai 2000). Cuomo (2015) find that soil erosion is indeed affected by the meteorological seasons. Therefore, it is necessary to reflect the rainfall erosivity factor of the study area more authentically through the seasonal rainfall data, and rainfall is the main factor inducing soil erosion (Cuomo and Della Sala 2013). In addition, VCIs of different seasons can be obtained based on the rapid acquisition of images and their timeliness to more truly reflect the soil erosion conditions in different periods of the year. On the other hand, the conservation practices factor is expressed with some empirical values in empirical models and does not consider the slope angle, which has an important effect on conservation practices. The larger the slope angle is, the more obvious the influence of the slope factor on the conservation practices effect (Jiang et al. 2015; Li et al. 2010; Zhou et al. 2014). Hence, it is necessary to propose a new more accurate and reasonable conservation practices factor combining slope factors with conservation practices factors. In summary, a seasonal and slope-based RUSLE (SUSLE) model is proposed by simultaneously considering the effect of slope factors as well as the influence of seasonal factors on rainfall and VCIs.

The SUSLE model proposed in this study will be used to quantitatively predict soil erosion in Ningdu County, Jiangxi Province, China. This is because Ningdu County is a mountainous and hilly area under the influence of a typical subtropical monsoon climate, and soil erosion is one of the geological disasters that concern the local people. Then, the soil erosion prediction results of the SUSLE model and the RUSLE model are compared to analyze the application effect of the SUSLE model under the comprehensive action of seasonal factors and slope factors, which can promote the progress of the regional soil erosion quantitative prediction research. The quantitative prediction of soil erosion will provide effective guidance for the local government of Ningdu County to implement policies for conservation practices.

Theoretical analysis of the SUSLE model

RUSLE model

The widely used RUSLE model is selected to calculate the soil erosion in the study area. The RUSLE model is suitable for predicting long-term annual soil erosion amounts and comprehensively considers the impacts of natural conditions and human activities on soil erosion (Renard et al. 1997). The empirical equation is expressed as:

$$A = R \times C \times K \times L \times S \times P_{\mathrm{RUSLE}} \quad (1)$$

where A is the average annual soil erosion amount per unit area ([t/(ha × year)], R is the rainfall erosivity factor ([(MJ × mm)/(ha × h × year)]), C is the annual cover and management factor, K is the soil erodibility factor ([(t × ha × h)/(MJ × ha × mm)]), L is the slope length factor, S is the slope steepness factor, and P_{RUSLE} is the conservation practices factor without considering the effect of slope. The parameters L, S, C, and P_{RUSLE} are all dimensionless.

Seasonal and slope factor-based RUSLE model

The SUSLE model is used to consider the effects of rainfall and the VCI combination on soil erosion at different seasons in a year. SUSLE can be expressed as:

$$A = \sum_{i=1}^{i=4} R_i \times C_i \times K \times L \times S \times P_{\mathrm{SUSLE}} \tag{2}$$

where R_i is the seasonal rainfall erosivity factor ([(MJ × mm)/(ha × h × year)]), C_i is the seasonal cover and management factor, and P_{SUSLE} is the conservation practices factor considering the effect of slope; C_i and P_{SUSLE} are dimensionless. The factors of the RUSLE and SUSLE models are unified into a grid layer in the WGS84 coordinate system with a grid cell resolution of 30 m, and the soil erosion classification map of Ningdu County is generated by multiplying the factors.

The factors of the RUSLE and SUSLE models

The factors of the RUSLE and SUSLE models include rainfall, soil erodibility, topography, vegetation cover, and management factors. These environmental factors are the key factors affecting the soil erosion prediction performances of the RUSLE and SUSLE models.

Rainfall erosivity factor

The rainfall erosivity factor R represents the potential capacity of soil erosion caused by rainfall, which quantifies the splash effect of raindrops and indicates the erosion and transport capacities of runoff (Cuomo et al. 2016; Kinnell 2019; Risal et al. 2016). The typical calculation method is that of Wischmeier (1976) who calculated the rainfall erosivity index (EI_{30}) by multiplying the rainfall kinetic energy (E) and the maximum 30-min rainfall intensity (I_{30}). Some simple algorithms have also been proposed due to the difficulty in obtaining data on the subrainfall process. For example, Zhang et al. (2002) proposed a simple algorithm of rainfall erosivity based on daily rainfall data. Yu and Rosewell (1996) proposed a simple model for estimating the monthly rainfall erosion based on the daily rainfall data in Australia.

In this study, the rainfall erosivity was estimated by using Wischmeier's method based on the annual and monthly average rainfall (Wischmeier and Cross, 1971) as:

$$R = \sum_{i=1}^{i=12} \left\{ 1.735 \times 10^{\left(1.5 \times \lg \frac{p_i^2}{p} - 0.8188\right)} \right\} \tag{3}$$

where p_i is the monthly average rainfall (mm) for the month i, p is the annual average rainfall (mm), and R represents the annual average rainfall erosivity value. According to Eq. (3), the annual average and seasonal average rainfall erosivity of each station are calculated by using the monthly average rainfall data from 8 meteorological stations in and around Ningdu County from 1998 to 2017, and the annual average rainfall erosivity is the sum of the 12 monthly rainfall erosivity, and the seasonal average rainfall erosivity is the sum of the corresponding monthly rainfall erosivity. The inverse distance weighting (IDW) interpolation method is used to obtain continuous R factor maps of the RUSLE and SUSLE models in the whole study area.

Soil erodibility factor

The soil erodibility factor (K) measures the susceptibility of surface soil to rainfall splash erosion and runoff erosion transport. Parameter K is an important index to evaluate the erodibility of the soil itself (Buttafuoco et al. 2011). The nomograph is a commonly used method to calculate the K value (Addis and Klik 2015). The soil erodibility nomograph is drawn based on soil permeability; structure class; and the percentages of silt, sand, and organic matter (OM). However, the nomograph cannot be directly used to calculate the K value due to the lack of regional data about the structure coefficient and the permeability level. To address this problem, the erosion productivity impact calculator (EPIC) is adopted to obtain a K value, as shown in Eq. (4) (Sharpley and Williams 1990). In addition, Zhong and Zhong (2011) calculated the soil erodibility values of red soil and purple soil widely distributing in the Jiangxi Province to be 0.3252 and 0.2763 respectively under an artificial simulated rainfall experiment method using the USLE model, while to be 0.3138 and 0.2668 respectively using the EPIC method. The correction coefficient of EPIC is calculated to be 1.04 through comparing the soil erodibility factors calculated by using the above two methods. Therefore, the EPIC method is appropriate for calculating the K values in Jiangxi Province. Then, the K factor map of this study used for the RUSLE and SUSLE models is obtained by using the data interpolation method in the GIS software. The EPIC method is expressed as:

$$K = \left\{0.2 + 0.3\exp\left[-0.0256S_a\left(1-\frac{S_i}{100}\right)\right]\right\} \times \left(\frac{S_i}{C_l + S_i}\right)^{0.3} \left[1-\frac{0.25C}{C+\exp\left(3.718-2.947C\right)}\right] \times \left[1-\frac{0.7S_n}{S_n+\exp\left(-5.51+22.9S_n\right)}\right] \quad (4)$$

where S_a, S_i, C_l, and C are the percentage contents of sand, silt, clay, and organic carbon, respectively; S_n equates to $1 - S_a/100$; and C is equal to organic matter content divided by 1.724.

Topographic factor

The topographic factor is an index used to measure the impact of topographic and geomorphic features on soil erosion, which determines the speed of surface runoff, flow rate, and the intensity of material and energy conversion (Belasri and Lakhouili 2016). Slope length (L) is defined as the horizontal projection distance from the slope source point along the direction of runoff to the place where deposition occurred (Zhang et al. 2017). The longer the slope length, the greater the runoff. At the same time, the steeper the slope, the faster the runoff velocity; hence, the slope length is a direct factor affecting soil erosion (Xue et al. 2018). In general, the RUSLE model is more appropriate in areas with gentle slopes less than 10°. However, approximately 41.7% of Ningdu County is covered by areas with slopes greater than 10° (Fig. 2b). Therefore, the McCool formula is used to calculate the topographic factor (S) in the area with slopes less than 10° (McCool 1987), while the Liu Baoyuan formula is used for areas with slopes greater than 10° (Lui et al. 1994).

$$S = \begin{cases} 10.8\sin\theta + 0.03 & (\theta < 5°) \\ 16.8\sin\theta - 0.5 & (5° \le \theta < 10°) \\ 21.91\sin\theta - 0.96 & (\theta \ge 10°) \end{cases} \quad (5)$$

where S is the slope steepness factor and θ is the slope angle. The slope length factor is calculated by using the formula put forward by Liu Baoyuan (Lui et al. 1994):

$$L = (\lambda/22.13)^m \quad (6)$$

$$m = \begin{cases} 0.2 & (\theta \le 1°) \\ 0.3 & (1° < \theta \le 3°) \\ 0.4 & (3° < \theta \le 5°) \\ 0.5 & (\theta \ge 5°) \end{cases} \quad (7)$$

where L is the slope length factor, λ is the slope length, and m is the variable slope length exponent. The LS factor map calculated in Eq. (6) is used both in the RUSLE and SUSLE models.

Vegetation cover and management factor

The coverage and management factor (C) is defined as the ratio of the soil erosion amount of a particular crop to the soil erosion amount of a continuous fallow field under the same conditions (Hancock et al. 2017). In general, C values vary between 0 and 1 (Li et al. 2010). The inhibitory effect of vegetation on soil erosion can be reflected as that, the kinetic energy of raindrops is weakened through interception by the vegetation canopy of the flow rate of runoff is reduced by deciduous decay on the surface, and the root systems of dense plants have a strong soil fixation ability (Heng kai et al. 2014).

In addition, the C factor is closely related to land use type and vegetation coverage. Currently, it is widely used to obtain C factors through the normalized difference vegetation index (NDVI) for reflecting VCIs (Seeber et al. 2010; Shi et al. 2004):

$$C = \begin{cases} 1 & (f_c = 0) \\ 0.6508 - 0.3436\lg f_c & (0 < f_c \le 78.3\%) \\ 0 & (f_c > 78.3\%) \end{cases} \quad (8)$$

$$f_c = (\mathrm{NDVI} - \mathrm{NDVI_{min}})/(\mathrm{NDVI_{max}} - \mathrm{NDVI_{min}}) \quad (9)$$

where f_c is the vegetation coverage (%), NDVI represents the VCIs and the vegetation growth status in a grid cell, and $\mathrm{NDVI_{min}}$ and $\mathrm{NDVI_{max}}$ represent the smallest and largest NDVI values, respectively. The average annual and seasonal C factor maps under the RUSLE and SUSLE models were obtained by acquiring the representative NDVI vegetation products in March, July, October, and December 2017.

Conservation practices factor

The conservation practices factor (P) is defined as the ratio of soil erosion amount in an area carrying out specific conservation practices to the soil erosion amount in the same area planting under natural conditions (Bagherzadeh 2012;

Table 1 Conservation practices factor P_{SUSLE} of different slopes and land use types

Slope range	0~5°	5~10°	10~20°	20~30°	≥ 30°
Agriculture	0.05	0.1	0.2	0.25	0.25
Forest	0.4	0.5	0.6	0.7	0.8
Bare grass	0.8	0.85	0.9	0.95	1
Settlement	0	0.02	0.05	0.08	0.1
Waterbody	0				

Ganasri and Ramesh 2016). Its value is between 0 and 1, with 0 showing almost no erosion in this area and 1 indicating no conservation practices. The commonly used conservation practices are contour tillage, contour strip tillage, and building terraced fields, which reflect inhibiting effects on soil erosion.

Generally, the value of P is obtained by referring to local experiments. Because there is no runoff plot experiment in the study area, the P values are determined by referring to relevant literature in the study area based on the land cover map obtained by remote sensing classification and manual interpretation. Traditionally, P values are assigned with no consideration of the slopes, which reduces the accuracy of the P values. To overcome this problem, we performed an overlay analysis of the land cover map and the slope map to obtain more accurate P values (P_{SUSLE}) of the study area due to the influence of slope on the conservation practices factor (Hui et al. 2010; Karamage et al. 2016; Lu et al. 2011; Shi et al. 2004; Zhu 2014). The relationship between the P_{SUSLE} values and the land use and slope is shown in Table 1. The P_{RUSLE} map of this study is directly related to the land use in the RUSLE model, in which agriculture in the research area is 0.15, forest and bare grass is 1, settlement is 0.01 and waterbody is 0 (Chen et al. 2015; Irvem et al. 2007; Liangsong et al., 2015; Vezina et al. 2006; Zhou et al. 2014).

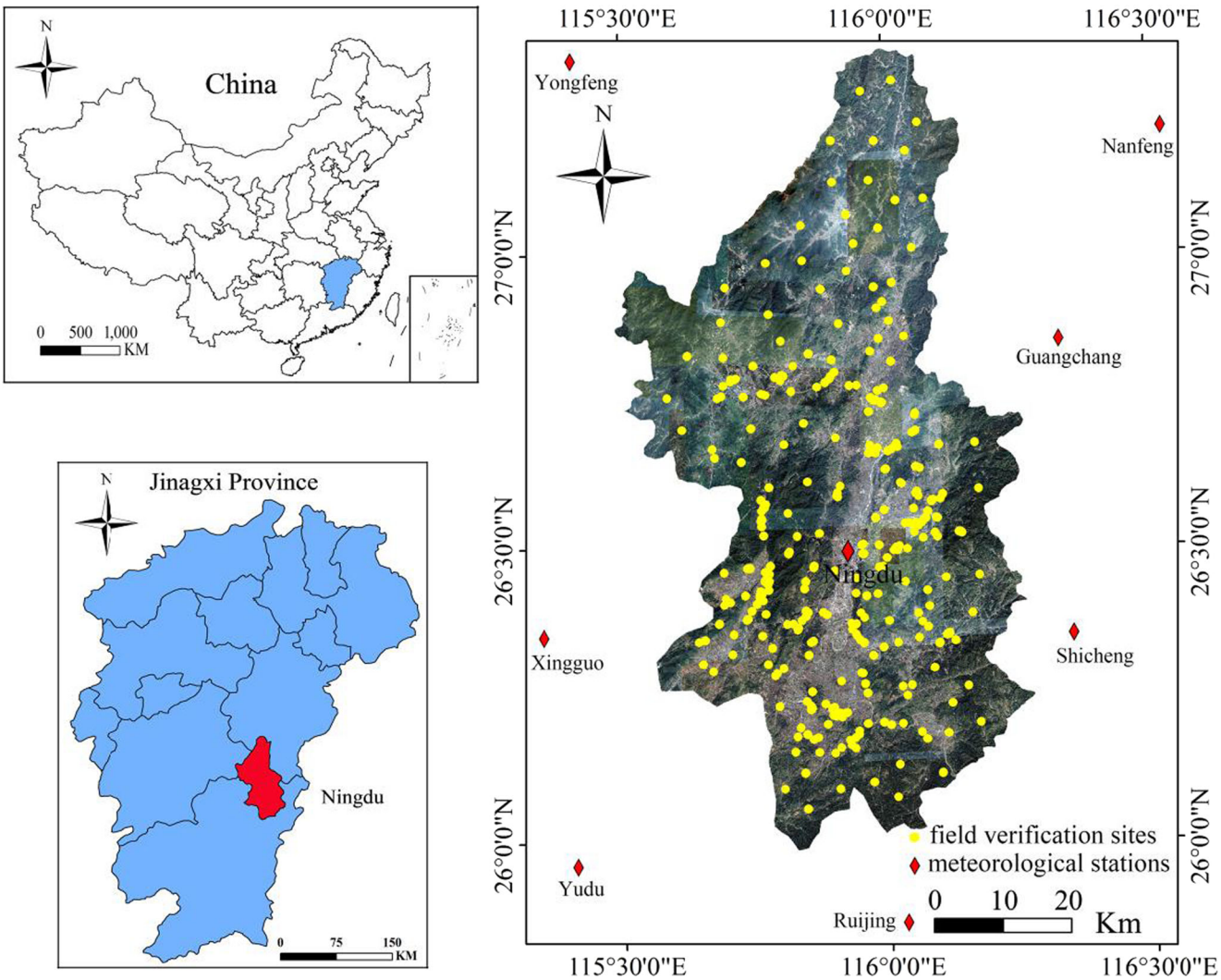

Fig. 1 Eight meteorological stations and typical verification sites in Ningdu County

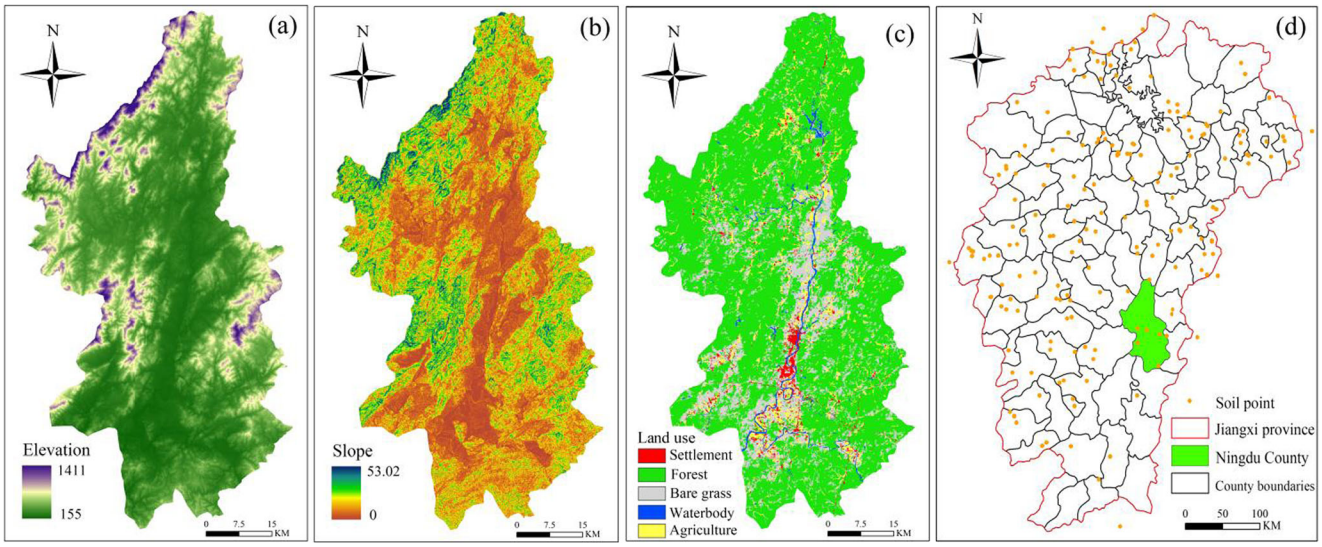

Fig. 2 Related environmental factors. **a** Elevation. **b** Slope. **c** Land use. **d** Soil sample distribution map in Jiangxi Province

Study area and date sources

Introduction of Ningdu County

Ningdu County (26° 05′~27° 08′ N, 115° 40′~116° 17′ E) is located north of Ganzhou City in southeastern Jiangxi Province, with a total area of 4075.45 km^2 (Fig. 1). Ningdu County has hilly and mountainous terrain. Its territory is mountainous in the north and is hilly in the middle. The elevation of Ningdu County is high in the north and low in the south, with an altitude of 154~1410.7 m. Ningdu County belongs to the humid subtropical zone with a monsoonal climate, with an average annual temperature of 14~19 °C and an average annual precipitation of 1500~1700 mm from the 1970s to 2015. The forest coverage rate in Ningdu County is approximately 71.8%, and the natural forest area accounts for approximately 87% of the forest area. The zonal vegetation is the central Asian zone evergreen broad-leaved forest.

Ningdu County is a typical red soil erosion area in the hilly areas of South China, where soil and water erosion need to be considered. Due to the rich mineral and rare earth resources in the research area and the need for economic development, the phenomenon of soil erosion is caused by frequent human activities and extensive mining and deforestation. Therefore, the study of soil erosion has important practical significance for sustainable and ecological land development in Ningdu County.

Table 2 The location and average monthly rainfall of the eight stations in the study area

Station name	Yudu	Nanfeng	Xingguo	Yongfeng	Ningdu	Guangchang	Shicheng	Ruijing
Site code	58905	58718	58804	58705	58806	58813	58814	58903
Longitude	115.41	116.53	115.35	115.41	116.01	116.33	116.35	116.03
Latitude	25.96	27.21	26.35	27.33	26.48	26.85	26.35	25.86
Elevation	132	111	147	85	209	143	229	193
Jan.	58.48	58.41	67.11	60.86	80.65	81.96	84.97	94.66
Feb.	82.09	66.88	48.28	83.17	65.87	68.35	71.06	72.35
Mar.	219.39	170.22	142.15	200.64	191.99	221.74	203.48	184.7
Apr.	202.65	187.87	128.55	191.28	199.96	198.22	200.98	187.06
May	239.98	235.83	181.67	248.87	315.36	309.74	306.6	309.55
Jun.	259.42	298.26	237.99	319.81	333.67	290.8	309	314.43
Jul.	205.05	147.9	132.81	180.32	170.33	124.16	149.05	131.65
Aug.	121.55	123.4	202.61	133.41	166.24	145.14	189.23	174.95
Sep.	101.96	96.76	115.3	85.59	77.57	73.23	87.67	82.73
Oct.	56.28	58.66	61.84	54.43	53.29	42.46	51.57	42.56
Nov.	126.24	130.39	126.75	140.41	152.83	155.51	129.32	116.72
Dec.	76.36	76.93	63.21	76.87	74.61	79.53	83.01	73.24
Average annual rainfall	1749.45	1651.51	1508.27	1775.66	1882.37	1790.84	1865.94	1784.6

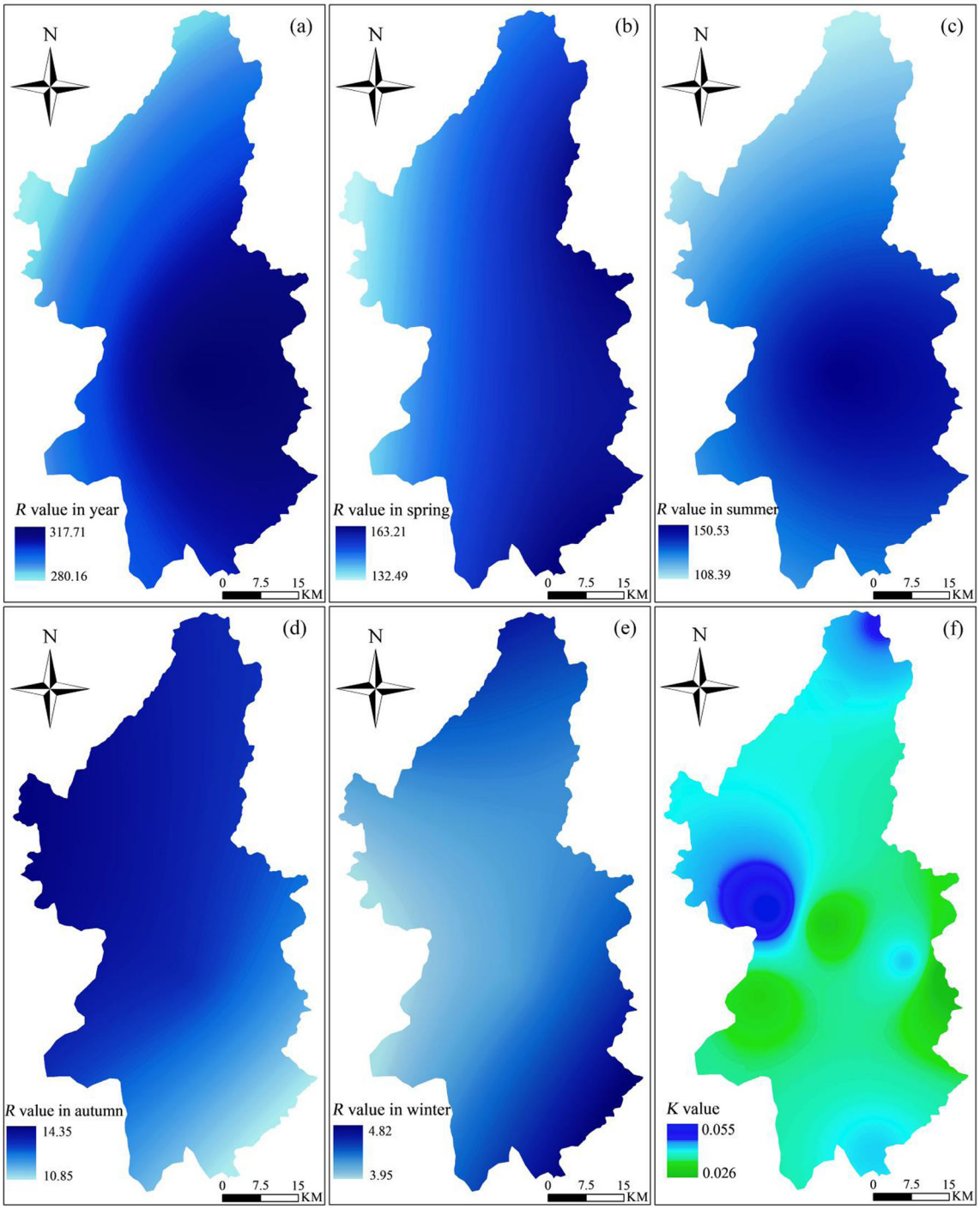

Fig. 3 RUSLE and SUSLE factors. **a** *R* in year. **b** *R* in spring. **c** *R* in summer. **d** *R* in autumn. **e** *R* in winter. (f) *K* in Ningdu County

Data sources and analysis

The basic data sources used in this study include:

1). DEM data with a resolution of 30 m is obtained from Google Earth 7.1.8.3036 (32-bit);
2). Land use map obtained from Landsat TM remote sensing image taken on December 19, 2017 with geometric precision correction and registration through the combination of remote sensing classification extraction and manual interpretation (Fig. 2c). The related Landsat TM remote sensing image is downloaded from the website of "http://ids.ceode.ac.cn/index.aspx." Land use is mainly divided into five types of forest, agricultural, settlement, bare grass, and water (Chang et al. 2020);

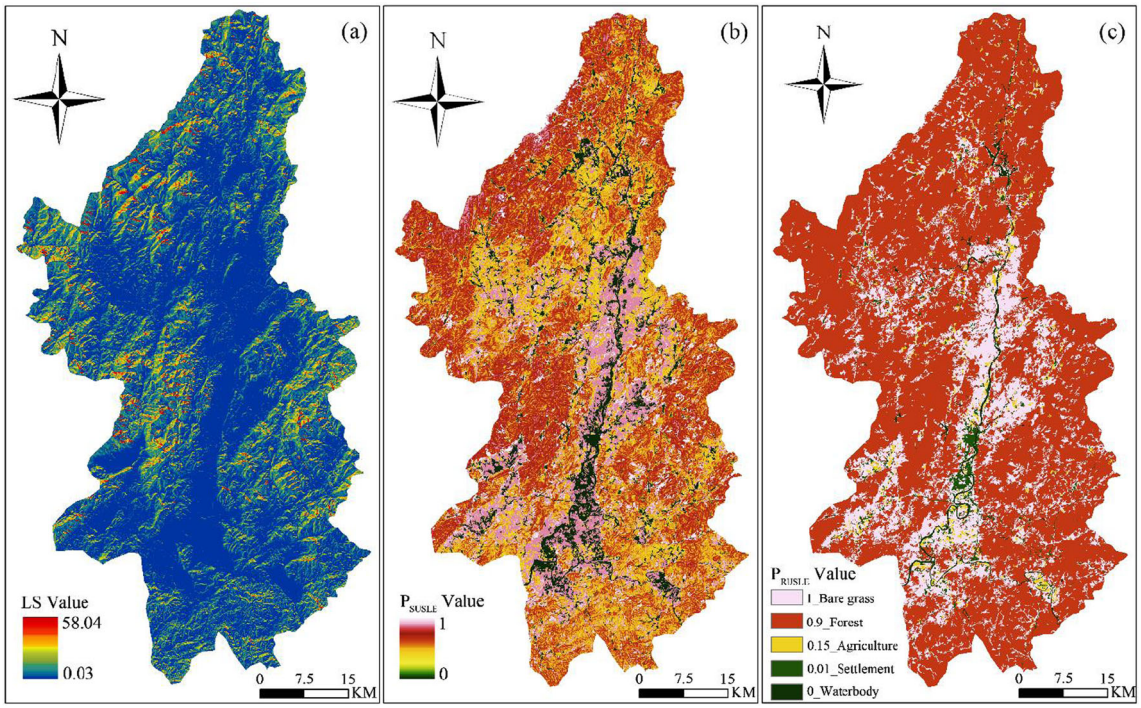

Fig. 4 RUSLE and SUSLE factors. **a** *LS*. **b** P_{SUSLE}. **c** P_{RUSLE}

3). Daily rainfall data of eight meteorological stations in or around the study area from 1998 to 2017 is shown in Fig. 1. These rainfall data is downloaded from China meteorological data center (http://data.cma.cn/); meanwhile, all the station locations and the average monthly rainfall are shown in Table 2;

4). The *K* values map of the study area shown in Fig. 3(f) is directly produced through interpolation analysis of the *K* values at the 194 soil points in Jiangxi Province (Fig. 2d) calculated by Renlin (2010) as shown in Fig. 2(d). In general, the red soil with high erodibility, paddy soil with low erodibility, and tidal soil with moderate erodibility are mainly distributed in the northwest, middle, and south part of the study area, respectively.

5). All the four NDVI maps are respectively calculated from the Landsat TM remote sensing images taken on March 12th, July 28th, October 3rd, and December 19th of 2017, which are also downloaded from the

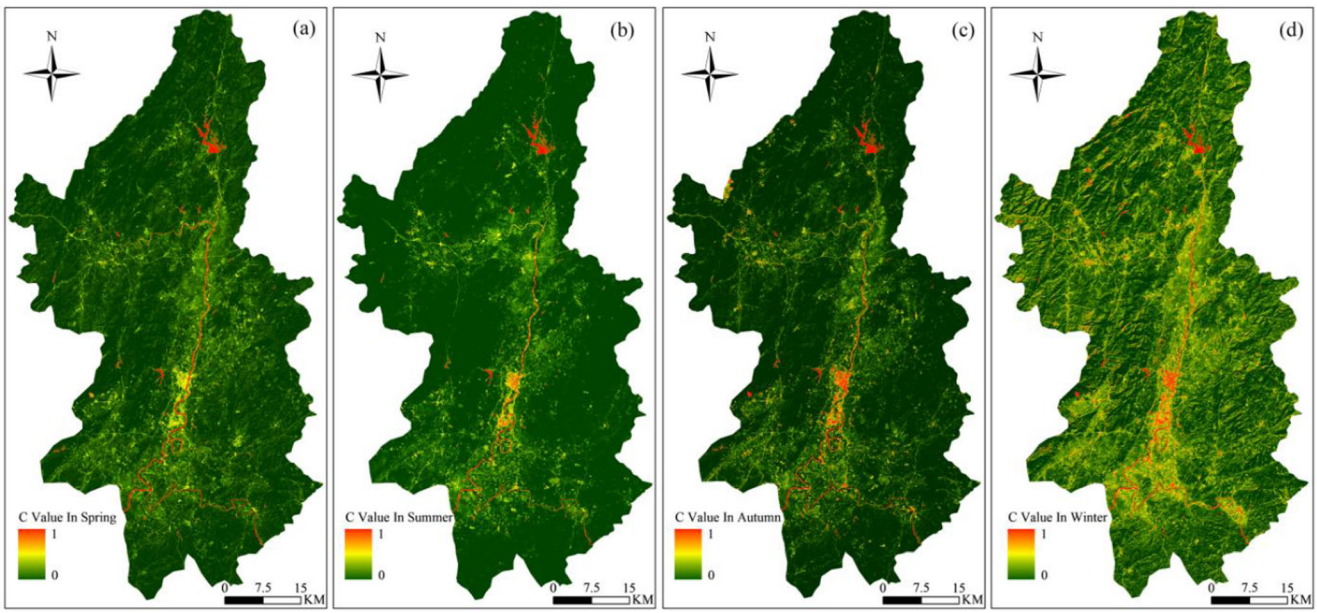

Fig. 5 Vegetation cover and management factors. **a** In spring. **b** In summer. **c** In autumn. **d** In winter

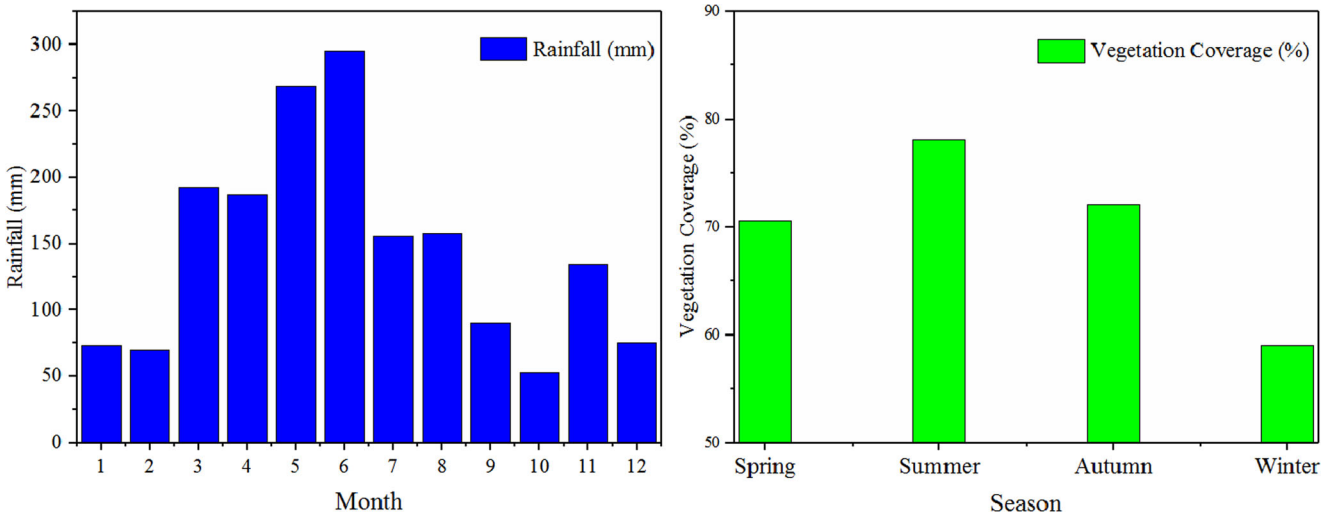

Fig. 7 Rainfall and vegetation cover changes in Ningdu County

website of "http://ids.ceode.ac.cn/index.aspx." Furthermore, these NDVI values are calculated in the ENVI 5.3 software using the above Landsat TM images as Eq. (10), where *NIR* and *R* indicate respectively the near-infrared band and red band of Landsat TM image (Huang et al. 2020; Huang et al. 2018; Zhu et al. 2020).

$$\mathrm{NDVI} = (NIR - R)/(NIR + R) \tag{10}$$

6). Part of the verification sites identified through high-resolution remote sensing images and/or field investigation is shown in Fig. 1. The grid resolutions of all factors are resampled to be 30 m with WGS84 coordinates in the ARCGIS 10.2 software.

Rainfall erosivity and soil erodibility factors of Ningdu County

Figure 3 shows that the distribution of *R* values has relatively high spatial differences with small *R* values in the northwest

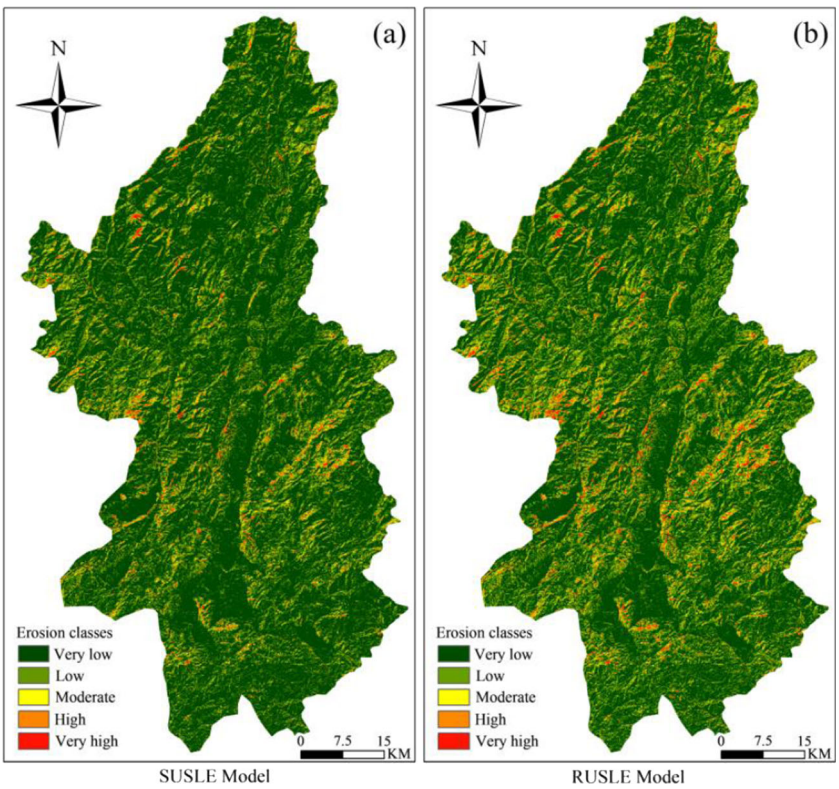

Fig. 6 Soil erosion classes in the SUSLE and RUSLE models of Ningdu County. **a** soil erosion classes in the SUSLE model. **b** Soil erosion classes in the RUSLE model

Table 3 Soil erosion class statistics in Ningdu County by using the SUSLE and RUSLE models in 2017

Erosion classes	Erosion modulus (t/ha/year)	SUSLE		RUSLE	
		Erosion area (km^2)	Erosion amount (10^4 t)	Erosion area (km^2)	Erosion amount (10^4 t)
Very low	< 5	2953.56	31.51	3018.88	28.32
Low	5–25	819.96	96.16	674.92	81.03
Moderate	25–50	194.08	67.39	205.52	72.39
High	50–80	64.84	40.25	88.19	55.27
Very high	> 80	43.01	59.29	87.94	146.23

and high *R* values in the southeast. The *R* values generally increase from northwest to southeast, and there are also obvious time differences. The highest *R* values mainly occur in the spring season, followed by the summer season, the autumn, and then the winter (Fig. 3 b, c, d, and e). The labels for color legend in Fig. 3(a~e) are the same. Meanwhile, the higher values of the soil erodibility factor (*K*) are mainly distributed in the northwest part of the study area due to the red soil with higher erodibility distributed in the northwest, while the smaller values of the *K* factor are mainly distributed in the central and eastern regions (Fig. 3f). The values of the *K* factor exhibit an overall trend of decreasing and then increasing from the northwest to the southeast.

Topographic and conservation practices factors in Ningdu County

The larger values of the *LS* factor are mainly distributed in the mountains around the research area, especially in the area with steep slopes, while the smaller values are mainly distributed near the convergence of water flow in the middle of Ningdu County (Fig. 4a). It can be seen from Fig. 4(b and c) that bare land and grassland with relatively large *P* values are mainly distributed in the middle and southwest regions of Ningdu County. Though considering the effects of topographic conditions on the conservation practices factor in the study area, the P_{SUSLE} map can more truly reflect the influence of slope on the conservation practices factor and their spatial distribution characteristics than the P_{RUSLE} map. The higher the slope is, the poorer the effects of the conservation practices. At the same time, the higher the vegetation cover is, the less the influence of slope on the conservation practices. Moreover, for sloping farmland, slope has a high effect on the conservation practices due to the influence of human activities.

Vegetation cover and management factors in Ningdu County

It can be seen from Fig. 5 that the seasonal distribution characteristics of the VCIs are obvious. The *C* values in summer are relatively high, and the *C* values in winter are significantly smaller than those in the other three seasons (Fig. 7). The zones with large *C* values are mainly distributed in the surrounding mountainous areas with dense vegetation and in areas with fewer human activities. In general, high VCIs have a greater inhibitory effect on soil erosion.

Results and discussion

General distribution characteristics of soil erosion

The soil erosion amounts in Ningdu County using the SUSLE and RUSLE models are calculated based on the factor layers through a map algebraic raster in the spatial analysis function of ArcGIS 10.2. Moreover, according to the Technological Standard of Soil and Water Conservation (SL190-2007) (Ministry of Water Resources 2008), the soil erosion class map can be revealed by classifying the soil erosion values into five corresponding erosion levels: very low, low, moderate, high, and very high (Fig. 6). The statistical analysis results (Table 3) show that the total annual erosion amount values of the SUSLE (Eq. (2)) and RUSLE (Eq. (1)) models are 2.946 million t and 3.832 million t, respectively, with an average of 3.389 million t. The soil erosion modulus values predicted by using the SUSLE and RUSLE models are respectively 722.870 t/km^2 and 940.370 t/km^2 in Ningdu County, which indicate that the soil erosion level in Ningdu County belongs to the low class according to the standard of SL190-2007. In addition, some studies have shown that the average annual soil erosion modulus in Ganzhou City, Jiangxi

Table 4 Sediment transport in Ganjiang river basin from 2005 to 2017 (unit/10^4 t)

Site	2005	2006	2007	2008	2009	2010	2011	2012	2013	2014	2015	2016	2017
Ganjiang basin	448	451	221	219	169	484	111	301	166	152	182	294	142

Table 5 Consistency of each erosion class in the RUSLE model and the SUSLE model

Erosion classes	RUSLE			SUSLE		
	Consistent points	Inconsistent points	Accuracy (%)	Consistent points	Inconsistent points	Accuracy (%)
Very low	339	58	85.39	359	38	90.43
Low	142	53	72.82	159	36	81.54
Moderate	79	18	81.44	83	14	85.56
High	85	22	79.44	90	17	84.11
Very high	74	30	71.15	84	20	80.77
Total	719	181	79.89	775	125	86.11

Province, China, is 1386.66 t/km^2 (Li et al. 2016); the average soil erosion modulus in the Poyang Lake watershed, Jiangxi Province, China, is approximately 1100 t/km^2 (Lu et al. 2011); and the average annual soil erosion modulus in Xingguo County, Ganzhou City, Jiangxi Province, China, is 1845.31 t/km^2 (Shi et al. 1996). Human activities and vegetation coverage are the main factors leading to different degrees of soil erosion. The different land cover types under different vegetation cover and soil erosion class distribution characteristics are important reasons for the annual average soil erosion modulus varying greatly on different regional scales. Ningdu County has a similar soil erosion modulus in or near the above study area.

Furthermore, Ganjiang river originates from the Meijiang river in the north part of Ningdu County, and the sediment concentration of Ganjiang river is closely related to the soil erosion level in Ningdu County. Therefore, the change rules of the sediment discharge transported by Ganjiang river reported by the institute of soil and water conservation of Jiangxi Province from 2005 to 2017 can be used to reflect the soil erosion level changes of Ningdu County (Table 4). It can be seen from Table 4 that although abnormal sediment discharge occurred in 2010, 2012, and 2016 due to flood disasters, the sediment discharge transported by Ganjiang river decreases gradually from 2005 to 2017 as a whole. This phenomenon indicates the decrease of soil erosion amount in the Ningdu County to some extent.

It can also be seen from Fig. 6 that the soil erosion distribution characteristics of the study area under the two models are similar to each other. The soil erosion levels calculated by both models belong to low soil erosion levels on the whole. The areas with high and very high soil erosion levels are mainly distributed in the northwest and east parts of Ningdu County. In addition, the severe soil erosion area obtained by using the SUSLE model is smaller than that obtained by using the RUSLE model. From the superposition and correlation analysis of the soil erosion class map with the soil erodibility factor map and the terrain factor map, it can be shown that the high soil erodibility factor and complex topographic factor have strong correlations with the high soil erodibility zones.

Table 6 Erosion area under different soil erosion moduli in different seasons

Erosion modulus (t/ha/year)	Area (km^2)			
	Spring	Summer	Autumn	Winter
0~2	2800.09	3433.15	4003.74	3987.03
2~5	443.58	315.17	58.61	73.95
5~10	313.91	146.36	9.53	12.07
10~20	268.08	96.71	2.51	2.34
20~35	144.02	45.94	0.79	0.06
> 35	105.77	38.12	0.27	0

Comparison of the RUSLE and SUSLE models

Approximately 900 randomly selected sites were verified through high-resolution remote sensing images and/or field investigation in Ningdu County in April~June 2018 (Fig. 6). About 300 verification sites classified as low and above soil erosion levels in the mountainous areas with bare grassland are shown in Fig. 1. The soil erosion classes were compared and verified with the classification classes calculated by using the RUSLE and SUSLE models in 2017 (Table 5). It can be seen from Table 5 that the accuracy distribution rule of all predictive soil erosion classes of the two models is basically similar with each other. The accuracy of the low and very high soil erosion classes is lower than the accuracies of the other classes, and the accuracy of the very low soil erosion class is the highest. In addition, the consistency of the SUSLE model at each class is higher than that of the RUSLE model, and the total accuracies of the RUSLE model and the SUSLE model are 79.89% and 86.11%, respectively, where it is the total number of correct points in classification levels, and it can represent the quality of the model prediction to some extent. Hence, it is concluded that the SUSLE model is more accurate in predicting soil erosion than the RUSLE model.

Table 7 Distribution of soil erosion in Ningdu County on different slopes

Slope classification (°)	Area (km^2)					Erosion area ratio (%)	Erosion amount (%)	Erosion modulus (t/km^2)
	Very low	Low	Moderate	High	Very High			
0~5	1238.67	88.11	3.6	0.48	0.36	32.67	6.57	145.28
5~8	458.39	167.49	24.66	7.25	3.77	16.23	14.46	643.91
8~15	735.07	331.3	59.71	15.36	9.66	28.24	31.03	794.24
15~25	429.59	204.26	88.07	28.34	14.81	18.77	34.11	1313.64
25~35	83.34	26.86	17.45	12.73	12.20	3.75	12.05	2326.67
> 35	8.5	1.94	0.58	0.67	2.23	0.34	1.78	3760.68

As seen in Fig. 6 and Table 3, the soil erosion areas of the two models are significantly different. The soil erosion areas of the SUSLE and RUSLE models are 1121.89 t/km^2 and 1056.57 t/km^2, respectively. The soil erosion areas calculated by using the SUSLE model in the moderate, high, and very high soil erosion classes are smaller, especially the high and very high soil erosion areas, which are approximately 26.47% and 51.09% smaller, respectively, than those calculated by using the RUSLE model. The annual total soil erosion amount of the RUSLE model is 23.13% larger than that of the SUSLE model. This is mainly because 71.67% of the rainfall is concentrated in March to August, and the VCIs are the largest in summer. Hence, the uneven distribution of the annual rainfall and the seasonal temporal change in the VCIs are the main reasons for the significant difference between the RUSLE and SUSLE models.

Effects of environmental factors on soil erosion distribution

Soil erosion distribution features affected by uneven rainfall and VCIs

The average monthly rainfall distribution and average seasonal VCIs in Ningdu County are shown in Fig. 7. As shown in Fig. 7, the change in rainfall is consistent with the change in the VCIs over time, which shows a trend of first increasing and then decreasing. The rainfall mainly occurs from March to August, accounting for 71.67% of the total rainfall during a year. The monthly rainfall ranges from 50 to 300 mm, with an average of 145.92 mm, among which the largest rainfall is 295.42 mm in June. For the values of the VCIs, the maximum value is in summer, and the lowest value is in winter, with an

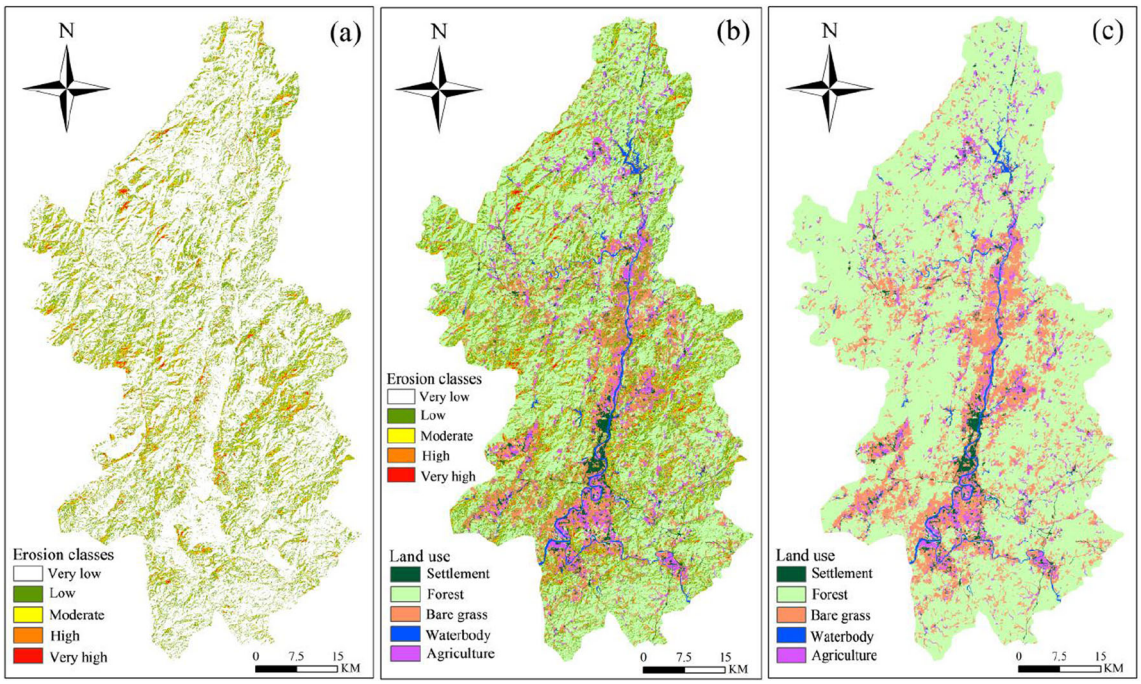

Fig. 8 Soil erosion classes (**a**). Land use and soil erosion overlay map (**b**). Land use map (**c**) of Ningdu County

Table 8 Soil erosion of different land use types

Land use types	Area (km^2)	Area ratio (%)	Erosion modulus (t/km^2)	Erosion amount (10^4 t)	Erosion amount ratio (%)
Forest	2926.69	71.81	355.62	104.08	35.33
Agriculture	375.26	9.21	1430.74	53.69	18.22
Bare grass	532.48	13.06	2529.48	134.69	45.72
Settlement	100.46	2.47	213.02	2.14	0.73
Waterbody	140.56	3.45	0	0	0

average value of 0.69. In addition, Fig. 5 clearly shows that the *C* value is the smallest in summer and is the largest in winter, which is consistent with the change in the VCIs.

Through the seasonal combination of the rainfall erosivity factors and the VCIs, the soil erosion amount in each seasonal period can be obtained based on the SUSLE model, and the soil erosion areas under different soil erosion moduli and different seasons are calculated as shown in Table 6. It can be seen from Table 6 that the difference in the soil erosion areas during different seasons is noticeable. Soil erosion mainly occurs in the spring and summer; furthermore, the area of soil erosion occurring in the spring with erosion modulus greater than 2 t/ha/year is 1275.36 km^2, larger than that in the summer, autumn, or winter. This is because the VCIs in summer are higher than those in spring under the same rainfall erosivity. In contrast, the area of erosion modulus greater than 2 t/ha/year in autumn is smallest with 71.71 km^2. The main reasons are that the vegetation cover rate in autumn is high and the rainfall is relatively low comparing with other seasons (Fig. 7).

Table 6 also shows that the seasonal soil erosion in Ningdu County varies greatly. Therefore, it is significant to fully consider the seasonal changes in rainfall and VCIs to understand the seasonal distribution characteristics of soil erosion and to improve the prediction accuracy of soil erosion (Cerdà 1998; Zhao et al. 2013).

Characteristics of soil erosion on different slopes

Soil erosion intensity has a strong correlation with topography (Fang et al. 2019). The overlapping analysis between the soil erosion class maps of the SUSLE model and the distribution layer of each factor shows that slope has a great impact on soil erosion. Moreover, the distribution of the soil erosion classes in different slope zones of Ningdu County is calculated clearly and shown in Table 7, suggesting that the soil erosion in Ningdu County is closely related to the slope distribution and suggests that the soil erosion modulus in Ningdu County increases with increasing slope. The distribution of the soil erosion classes obviously changes with the change in the slope zones. Very low soil erosion classes are mainly distributed in the area with slopes less than 5° (with an area of 1238.67 km^2); low, moderate, and high soil erosion classes are mainly distributed in the areas with slopes of 8~25°; and a very high soil erosion class occurs in the slope zone of 15~35°. The soil erosion area in the 0~5° zone is the largest, accounting for 32.67% of the study area, while the soil erosion amount accounts for only 6.57% of the total soil erosion amount and is mainly restricted by topographic factors. The soil erosion areas in the slope zone of 8~25° account for 47.01% of the total study area, with the soil erosion amount accounting for 65.14% of the total soil erosion amount, suggesting that slopes of 8~25° are the main slope section of soil erosion in the study area. In addition, the erosion amount in the slope zone of 25~35° (3.74% of the study area) accounts for 12.05% of the total soil erosion amount. Hence, in the study area, slopes of 8~25° are the key areas for predicted soil erosion and prevention.

Soil erosion characteristics under different land cover types

The superposition analysis of the present land use map and the soil erosion distribution map shows that the main land cover types in Ningdu County are forest, bare grass, and agriculture, accounting for 94.08% of the total area (Fig. 8). Among them, the forest area is the largest, accounting for 71.81%, mainly distributed in northwestern and eastern Ningdu County. Moreover, the settlement and waterbody erosion areas are small, mainly distributed in the central hilly area with flat central terrain, which is also the main region of human activities.

Table 8 shows that the soil erosion modulus in different land cover types has significant differences. For the settlement and waterbody land cover types, there is basically no soil and water loss. As the land cover type with the most serious effect on soil erosion, bare grass accounts for 13.06% of the total area and contributes to 45.72% of the total soil erosion amount. The soil erosion modulus for bare grass is the highest at 2529.48 t/km^2, which belongs to the moderate soil erosion level and is approximately 7 times greater than that in the area with forest land cover. Then, the soil erosion of agriculture in 9.21% of the total area contributes to 18.22% of the total soil erosion amount, and the soil erosion modulus is 1430.74 t/km^2.

In the study area, low levels of soil erosion mainly occur in the forest with relatively gentle slopes, mainly because there

are higher VCIs in this area, which can effectively reduce the soil erosion amount. The amount of soil erosion in some areas of agriculture increases, because the land cover type of agriculture changes to bare grass, wasteland, and other erosion-prone land types. The soil erosion with a moderate class mainly comes from bare grass, which is mostly natural grassland and is mainly distributed on wasteland with slopes less than 25°. The soil erosion in the area with settlement and waterbody land covers is within the permitted scope of soil erosion.

In general, the soil erosion amount in Ningdu County mainly comes from the bare grass in the moderate soil erosion class and the forest in the low soil erosion class, while the soil erosion in the agriculture area cannot be ignored. Therefore, to implement effective soil and water conservation, the bare grass should be changed into woodland, the agriculture should be changed into terrace or contour tillage, and the sparse woodland and artificial forest should be closed off.

Conclusions

Considering the effects of seasonal changes in the VCIs, the seasonal uneven rainfall, and the effects of slope on the conservation practices factor in 2017, this paper innovatively proposes a SUSLE model to quantitatively predict the soil erosion features in Ningdu County. The traditional RUSLE model is used as a comparative model. The investigation results show that the overall accuracy of the SUSLE model is 7.22% higher than that of the RUSLE model. It is calculated that the annual soil erosion amounts of the SUSLE and RUSLE models in Ningdu County are 2.946 million t and 3.824 million t, respectively, and the soil erosion moduli are 722.87 t/km^2 and 940.37 t/km^2, respectively. In addition, the soil erosion amounts in the areas with moderate, high, and very high soil erosion classes in the SUSLE model are smaller than those in the RUSLE model. The main types of soil erosion in Ningdu County belong to the very low and low classes, and low and moderate levels are the main sources of soil erosion. Meanwhile, soil erosion in a high class cannot be ignored.

The areas of soil erosion in different seasons vary significantly. The maximum soil erosion area occurs in spring, and the minimum area occurs in autumn. Meanwhile, in spring and summer, the influence of rainfall on soil erosion is greater than that of the VCIs. In contrast, the influence of the VCIs is greater than that of rainfall in autumn and winter. Soil erosion under different slope zones varies significantly in the study area, and the soil erosion modulus increases with increasing slope. In terms of soil erosion area and amount, the 8~25° slope zone, which is the main erosion slope zone and control zone, accounts for the largest proportion. In terms of land cover types, bare grass and agriculture are the main land types contributing to soil erosion in the study area.

Funding information This research is funded by the National Key Research and Development Program (NO. 2017YFC1502505); the National Natural Science Foundation of China (No.41807285, 41762020, 51879127, and 51769014); the National Science Foundation of Jiangxi Province, China (20192BAB216034, 20192ACB2102, 20192ACB20020); the Postdoctoral Science Foundation of China (NO.2019M652287); and the Jiangxi Provincial Postdoctoral Science Foundation (NO. 2019KY08).

References

Addis HK, Klik A (2015) Predicting the spatial distribution of soil erodibility factor using USLE nomograph in an agricultural watershed, Ethiopia. International Soil and Water Conservation Research 3(4): 282–290

Bagherzadeh A (2012) Estimation of soil losses by USLE model using GIS at Mashhad plain, northeast of Iran. Arab J Geosci 7(1):211–220

Baumann V, Bonadonna C, Cuomo S, Moscariello M (2020) Modelling of erosion processes associated with rainfall-triggered lahars following the 2011 cordon caulle eruption (chile). J Volcanol Geotherm Res:*390*

Belasri A, Lakhouili A (2016) Estimation of soil erosion risk using the universal soil loss equation (USLE) and geo-information technology in Oued El Makhazine watershed, Morocco. J Geogr Inf Syst 8(1): 98–107

Buttafuoco G, Conforti M, Aucelli PPC, Robustelli G, Scarciglia F (2011) Assessing spatial uncertainty in mapping soil erodibility factor using geostatistical stochastic simulation. Environ Earth Sci 66(4):1111–1125

Cai C (2000) Study of applying USLE and geographical information system IDRISI to predict soil erosion in small watershed. J Soil Water Conserv 14(2):19–24

Cao C, Sun Y, Sun H, Song Y (2018) Erosion resistance and scouring depth of fine-grained seabed of the Huanghe river estuary, China. Bull Eng Geol Environ 77(3):897–910

Cerdà A (1998) The influence of aspect and vegetation on seasonal changes in erosion under rainfall simulation on a clay soil in Spain. Can J Soil Sci 78(2):321–330

Chang Z, Du Z, Zhang F, Huang F, Chen J, Li W, Guo Z (2020) Landslide susceptibility prediction based on remote sensing images and GIS: comparisons of supervised and unsupervised machine learning models. Remote Sens 12(3):502

Chen YB, Liang JM, Wang SY (2015) The characteristics of spatial-temporal differentiation of soil erosion based on RUSLE model: a case study of Chaoyang city, Liaoning province. Sci Geogr Sin 35(3):365–372

Cuomo S, Della Sala M (2013) Rainfall-induced infiltration, runoff and failure in steep unsaturated shallow soil deposits. Eng Geol 162: 118–127

Cuomo S, Chareyre B, d'Arista P, Della Sala M, Cascini L (2016) Micromechanical modelling of rainsplash erosion in unsaturated soils by discrete element method. Catena 147:146–152

Dai Z, Huang Y, Xu Q (2019) A hydraulic soil erosion model based on a weakly compressible smoothed particle hydrodynamics method. Bull Eng Geol Environ:1–12

de Lollo JA, Sena JN (2013) Establishing erosion susceptibility: analytical hierarchical process and traditional approaches. Bull Eng Geol Environ 72(3–4):589–600

Fang G, Yuan T, Zhang Y, Wen X, Lin R (2019) Integrated study on soil erosion using RUSLE and GIS in Yangtze river basin of Jiangsu province (China). Arab J Geosci 12(5). https://doi.org/10.1007/s12517-019-4331-2

Ganasri BP, Ramesh H (2016) Assessment of soil erosion by RUSLE model using remote sensing and GIS-a case study of Nethravathi basin. Geosci Front 7(6):953–961

Hancock GR, Verdon-Kidd D, Jbc L (2017) Soil erosion predictions from a landscape evolution model-an assessment of a post-mining landform using spatial climate change analogues. Sci Total Environ 601-602:109

Heng kai LI, Liu XS, Bo LI, Fa shuai LI, Beijing T (2014) Vegetation coverage variations and correlation with geomorphologic factors in red soil region: a case in south Jiangxi province. Sci Geogr Sin 34(1):103–109

Huang F, Chen L, Yin K, Huang J, Gui L (2018) Object-oriented change detection and damage assessment using high-resolution remote sensing images, Tangjiao landslide, three Gorges reservoir, China. Environ Earth Sci 77(5):183

Huang F, Cao Z, Guo J, Jiang S-H, Li S, Guo Z (2020) Comparisons of heuristic, general statistical and machine learning models for landslide susceptibility prediction and mapping. CATENA 191:104580. https://doi.org/10.1016/j.catena.2020.104580

Hui L, Xiaoling C, Lim KJ, Xiaobin C, Sagong M (2010) Assessment of soil erosion and sediment yield in liao watershed, Jiangxi province, China, using USLE, GIS, and RS. J Earth Sci 21(6):941–953

Irvem A, Topaloglu F, Uygur V (2007) Estimating spatial distribution of soil loss over Seyhan river basin in Turkey. J Hydrol 336(1):30–37

Jiang L, Yao Z, Liu Z, Wu S, Wang R, Wang L (2015) Estimation of soil erosion in some sections of lower Jinsha river based on RUSLE. Nat Hazards 76(3):1831–1847

Kang G-o, Do TM, Lim J-s, Kim Y-s (2019) Evaluation of erosion resistance capacity on compacted weathered granite soil using non-destructive tests. Bull Eng Geol Environ:1–17

Karamage F, Zhang C, Kayiranga A, Shao H, Fang X, Ndayisaba F, Nahayo L, Mupenzi C, Tian G (2016) USLE-based assessment of soil erosion by water in the Nyabarongo river catchment, Rwanda. Int J Environ Res Public Health 13(8):835

Kinnell PIA (2018) Determining soil erodibilities for the USLE-MM rainfall erosion model. Catena 163:424–426. https://doi.org/10.1016/j.catena.2018.01.008

Kinnell PIA (2019) Determining soil erodibility for the USLE-MM rainfall erosion model (vol 167, pg 444, 2018). Catena 179:220–220. https://doi.org/10.1016/j.catena.2019.03.045

Lal R (2001) Soil degradation by erosion. Land Degrad Dev 12:519–539

Li H, Yang L, Lei J (2016) Soil erosion analysis in red soil hilly region by using HJ-CCD: a case study in Ganzhou. Remote sensing information. Remote Sensing Information 31(3):122–129

Liangsong Z, Guohui D, Jiachuang GU (2015) Dynamic changes of soil erosion in the Chaohu watershed from 1992 to 2013. Acta Geograph Sin

Liu W, Wan S, Huang F, Luo X, Fu M (2019) Experimental study of subsurface erosion in granitic under the conditions of different soil column angles and flow discharges. Bull Eng Geol Environ:1–12

Lu J, Chen X, Li H, Liu H, Xiao J, Yin J (2011) Soil erosion changes based on GIS/RS and USLE in Poyang lake basin. Transactions of the Chinese Society of Agricultural Engineering 27(2):337–344

Lui BY, Nearing MA, Risse LM (1994) Slope gradient effects on soil loss for steep slopes. Trans ASAE 37(6):1835–1842

McCool DK (1987) Revised slope steepness factor for the universal soil loss equation. Trans ASAE 30(5):1387–1396 Retrieved from https://ci.nii.ac.jp/naid/80003703585/en/

Ministry of Water Resources P R (2008) China (2008) soil erosion rate standard, technological standard of soil and water conservation sl190-2007. China Water Power Press, Beijing, pp 1–26

Mushi CA, Ndomba PM, Trigg MA, Tshimanga RM, Mtalo F (2019) Assessment of basin-scale soil erosion within the Congo river basin: a review. Catena 178:64–76. https://doi.org/10.1016/j.catena.2019.02.030

Pimentel D (2006) Soil erosion: a food and environmental threat. Environ Dev Sustain 8(1):119–137

Renard KG, Foster GR, Weesies GA, Mccool DK, Yoder DC (1997) Predicting soil erosion by water: a guide to conservation planning with the revised universal soil loss equation (RUSLE). Agricultural Handbook

Renlin Z (2010) Analysis of regional distribution of soil resistance index to erosion in Jiangxi province[d]. Changjiang academy of sciences, Wuhan

Risal A, Bhattarai R, Kum D, Park YS, Yang JE, Lim KJ (2016) Application of web erosivity module (WERM) for estimation of annual and monthly R factor in Korea. Catena 147:225–237

Seeber C, Hartmann H, Xiang W, King L (2010) Land use change and causes in the Xiangxi catchment, three Gorges area derived from multispectral data. J Earth Sci 21(6):846–855

Sharpley AN, Williams JR (1990) Epic-erosion/productivity impact calculator: 2. User manual Technical Bulletin - United States Department of Agriculture, 4(4), 206–207

Shi D, Shi X, Li D (1996) Study on dynamic monitoring of soil erosion using remote sensing technique. Acta Pedol Sin 33(1):48–58

Shi ZH, Cai CF, Ding SW, Wang TW, Chow TL (2004) Soil conservation planning at the small watershed level using RUSLE with GIS: a case study in the three Gorge area of China. Catena 55(1):33–48

Vezina K, Bonn F, Van CP (2006) Agricultural land-use patterns and soil erosion vulnerability of watershed units in Vietnam's northern highlands. Landsc Ecol 21(8):1311–1325

Wang L, Li X-A, Li L-C, Hong B, Liu J (2019) Experimental study on the physical modeling of loess tunnel-erosion rate. Bull Eng Geol Environ:1–14

Wischmeier WH (1976) Use and misuse of universal soil loss equation. J Soil Water Conserv 31(1):5–9

Wischmeier WJC, Cross B (1971) Soil erodibility nomograph for farmland and construction sites. J Soil Water Conserv 26(5):189–193 Retrieved from https://ci.nii.ac.jp/naid/10006070628/en/

Wischmeier WH, Smith DD (1978) Predicting rainfall erosion losses-a guide to conservation planning. Agric Handbook 537

Xue J, Lyu D, Wang D, Wang Y, Yin D, Zhao Z, Mu Z (2018) Assessment of soil erosion dynamics using the GIS-based RUSLE model: a case study of Wangjiagou watershed from the three Gorges reservoir region, southwestern China. Water 10(12):1817

Yu B, Rosewell CJ (1996) Technical notes: a robust estimator of the r-factor for the universal soil loss equation. Transactions of the ASAE, 39(2):559–561

Zhang W, Xie Y, Liu B (2002) Rainfall erosivity estimation using daily rainfall amounts. Sci Geogr Sin 22(6):705–711

Zhang H, Wei J, Yang Q, Baartman JEM, Gai L, Yang X, Li S, Yu J, Ritsema CJ, Geissen V (2017) An improved method for calculating slope length (λ) and the LS parameters of the Revised Universal Soil Loss Equation for large watersheds. Geoderma 308:36–45

Zhang HD, Zhang RH, Qi F, Liu X, Niu Y, Fan ZF, Zhang QH, Li JZ, Yuan L, Song YY et al (2018) The CSLE model based soil erosion prediction: comparisons of sampling density and extrapolation method at the county level. Catena 165:465–472. https://doi.org/10.1016/j.catena.2018.02.007

Zhang L, Wu F, Zhang H, Zhang L, Zhang J (2019) Influences of internal erosion on infiltration and slope stability. Bull Eng Geol Environ 78(3):1815–1827

Zhao X, Zhang B, Wu P (2013) Changes in key driving forces of soil erosion in the middle Yellow River basin: vegetation and climate. Nat Hazards 70(1):957–968. https://doi.org/10.1007/s11069-013-0849-x

Zhong R, Zhong P (2011) Calculation methods of soil anti-erodibility index of red soil and purple soil. Bulletin of Soil & Water Conservation 31(6):95–98

Zhou Q, Yang S, Zhao C, Cai M, Ya L (2014) A soil erosion assessment of the upper Mekong River in Yunnan province, China. Mt Res Dev 34(1):36–47

Zhu M (2014) Soil erosion assessment using USLE in the GIS environment: a case study in the Danjiangkou reservoir region, China. Environ Earth Sci 73(12):7899–7908

Zhu L, Huang L, Fan L, Huang J, Huang F, Chen J, Zhang Z, Wang Y (2020) Landslide susceptibility prediction modeling based on remote sensing and a novel deep learning algorithm of a cascade-parallel recurrent neural network. Sensors 20(6):1576 Retrieved from https://www.mdpi.com/1424-8220/20/6/1576